24th ABCM International Congress of Mechanical Engineering
December 3-8, 2017, Curitiba, PR, Brazil

COBEM-2017- 0808
EXPERIMENTAL STUDY OF A LEAN PREMIXED TURBULENT SWIRLING FLAME STABILIZATION

Luís Fernando Figueira da Silva
Carolina Sampaio Mergulhão
Letícia Piton
Pontifícia Universidade Católica do Rio de Janeiro, Department of Mechanical Engineering, Rio de Janeiro, Brazil.
luisfer@puc-rio.br
carol.mergulhao@hotmail.com
leticiacpiton@gmail.com

Philippe Scouflaire
Nasser Darabiha
Laboratoire EM2C, CNRS, CentraleSupélec, Université Paris-Saclay, Gif-sur-Yvette, France.
philippe.scouflaire@cnrs.fr
nasser.darabiha@centralesupelec.fr

Abstract. *Lean premixed turbulent combustion technologies often involve swirl-stabilized combustion, which exhibit the fundamental challenges of adequately predicting the combustor blow-off and flashback limits. Among the factors influencing the turbulent swirling flame and combustor behavior, the swirler and combustion chamber geometrical features are paramount. The present work is devoted to experimental characterization of the swirler geometry and the influenced combustion chamber confinement on blow-off characteristics and flame topologies of swirl-stabilized, premixed methane-air turbulent flames. A novel experimental test bench is first described, which allows for easily changing the radial swirler geometrical features and the combustion chamber confinement. Different flame shapes are shown to characterize the unconfined and confined flames, the latter exhibiting significant interactions with the combustion walls. The combustor blow-off limits are determined as functions of the mixture composition and flow rate. An important decrease of the blow-off equivalence ratio is observed when the flames are confined.*

Keywords: *experimental study, combustion instability, swirling flows, blow-off, confinement stability, flame topology.*

1. INTRODUCTION

Lean premixed turbulent combustion technologies are being pursued as effective means of reducing NOx and soot emissions in gas turbines and industrial burners. Such technologies, which often involve swirl-stabilized combustion, exhibit the fundamental challenges of adequately predicting the combustor blow-off and flashback limits, as well as the undesirable acoustic instabilities. Concerning the latter aspect, (Huang and Yang, 2009) presented a review of the interplay between the flow dynamics and the onset of combustion instabilities, with focus on the driving mechanisms and suppression techniques. An extensive discussion of experimental and modeling efforts was also carried out. More recently, (Candel, *et al*., 2014) reviewed swirling combustion state-of-the-art, with emphasis on the swirl number influence on the flow structure and on the instabilities onset. The results of non-linear flame and combustor dynamics analysis via a transfer function approach were also discussed. The interplay between the chemical time scales, that may lead to quenching and combustion induced vortex-induced breakdown, was studied by (Kröner, *et al*., 2007). The flashback limits were shown to be related to a quenching parameter for several operating conditions.

The effects of mixture equivalence ratio and flow rate on the observed combustion regimes, as well as associated mixing processes on a swirl burner, have been addressed by (Galley, *et al*., 2011). This work also proposed a formal order-of-magnitude analysis of the swirl number definition. As presented by (Chterev, *et al*., 2014), the results of an extensive experimental and numerical investigation of some of the factors that influence the four identified flame shapes, among which are the central bluff body geometrical shape and temperature, fuel/air ratio, mixture temperature. As demonstrated by (Terhaar, *et al*., 2014), steam dilution may also significantly alter the flame shapes observed and, thus, the resulting detailed flow structures. The experimental study of (Guiberti, *et al*., 2015) identified the role played by the swirl number on premixed H_2/CH_4/air turbulent flames. The studied flames, which exhibit strong interactions with the combustion chamber walls, were categorized as “M” and “V” flames. A topology transition model was developed and the effects of Lewis number and velocity gradient were identified. The influence of CO_2 and N_2 dilution on swirling CH_4/O_2 combustion was demonstrated by (Jourdaine, *et al.*, 2016). The swirl number and injector quarl angle effects on flame topology and stabilization were also investigated. Four different swirling turbulent flame shapes have been identified by (Foley, *et al.*, 2015). The transition between CH_4/H_2/air flame shapes was shown to be influenced by mixture equivalence ratio and hydrogen content. Among the flame shapes studies, some are significantly influenced by the interaction with the combustion chamber walls. Scaling laws have been proposed accounting for the different sound pressure levels within the combustor.

Three types of flashback mechanism were identified by (Sayad, et al., 2014), each of them was found to be influenced by the swirl number and/or the mixture equivalence ratio. The swirl number influence on CH_4/H_2/air turbulent flames flashback was evidenced in the experimental work of (Ebi and Clemens, 2016). This work examined the detailed mechanism leading to upstream flame propagation along the swirler boundary layer. A detailed study of the swirling premixed flame stability mechanisms was performed by (Foley, *et al*., 2015). Combined velocity and scalar measurements were used to assess the mechanisms related to flame blow-off, which seems to be related to the interplay between the instantaneous tangential velocity component and the flame edge speed.

The isothermal and reacting structures characteristics of turbulent swirling flows both with and without a cylindrical confinement were compared by (Khalil, *et al*., 2016). The effect of Reynolds number on the recirculating zone strength was demonstrated, as was the drastic effect of confinement on the turbulence intensity. A combined numerical and experimental study of isothermal and reactive swirling confined turbulent flows has been developed by (Orbay, *et al*., 2013). The effects of heat release and of the exit test section contraction on the flow field structure were demonstrated. The transition between different turbulent swirling flame types was explained using a Karlovitz number-based criterium, i.e., flames that lead to combustion within the outer recirculation zone or not. This Karlovitz number is based on the outer recirculating zone spinning frequency and extinction strain rate, and accounts for experimental results involving CH_4/H_2/air mixtures with different compositions, Reynolds number, swirler blade angle and heat loss. The studied flames seem to be strongly influenced by the confinement also. A numerical assessment of the confinement influence, with emphasis on the adequate representation of the combustor wall boundary conditions, was performed by (Nogenmyr, *et al*., 2013). In particular, the wall temperature distribution was shown to affect the ability of the large eddy simulation results to represent the measured velocity distribution. Large eddy simulation results obtained by (Bourgouin, *et al*., 2013) demonstrated how seemingly minute swirler geometry modifications may lead to rather large swirling flow field differences.

These works show that, among the factors influencing the turbulent swirling flame and combustor behavior, the swirler and combustion chamber geometrical features are paramount. Therefore, the present work is devoted to the experimental characterization of the swirler geometry and the combustion chamber confinement influence on the blow-off characteristics and flame topologies of swirl-stabilized methane-air turbulent premixed flames. To that end, a novel experimental test bench is first described, which allows for easily exchanging the radial swirler. Furthermore, the test bench design, which is based on the (Daguse, *et al*., 1996) also permits the assessment of the drastic influence of the confinement on flame stabilization. The flame blow-off characteristics will be shown to be influenced by the confinement cross section. The flame topological characterization is performed by both photography and CH* chemiluminescence.

2. EXPERIMENTAL SETUP AND METHODS

The novel experimental test bench used in the present study has been designed to permit swirler interchange and to accommodate two different combustion chamber section dimensions, which provide different degrees of confinement to the turbulent flame. Figure 1 presents the experimental test bench, which comprises the burner, the swirler, the confinement (combustion chamber), two flow meters (methane and air mixture), and a flow controller.

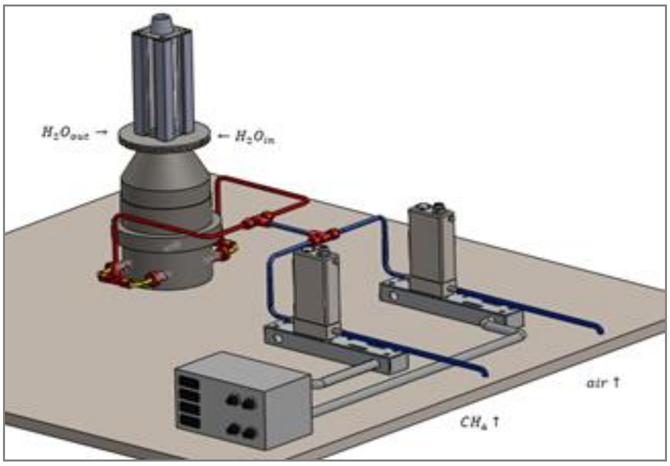

Figure 1. Experimental test bench scheme.

The flowmeter used for methane is a Bronkhorst mass flow controller (series F-201AC), which has maximum range of 138.9 cm^3/s with 0.5 % reading plus 0.1 % full scale uncertainty. The flowmeter control is made by an electronic device. The air volume flow rate is measured using a pair of rotameters (Omega, 4T70903X12 and 4T708TX12 models), which allow for a maximum flow rate of 1 dm^3/s and have a 2 % reading plus 2 % full scale uncertainty. The air flow temperature is measured using a type T thermocouple (Salvi Casagrande). In this study, the CH_4 flow rate varies from 6.9 cm^3/s to 66.8 cm^3/s and the air flow rates varies from 83.0 cm^3/s to 958.0 cm^3/s, thus leading to large variations equivalence ratio variation, between 0.46 and 1.6

2.1 Burner: swirler and confinement configurations

Figure 2 shows the two different stainless steel radial swirlers which are considered in this study. The fresh mixture swirling motion is induced by eight, 2 mm diameter, orifices, which axis are tangentially displaced 4 mm from the main swirler axis. These orifices feed a 10 mm diameter swirling chamber, which is 17 mm long. The central part of this chamber is occupied by a 4 mm diameter cylinder, which is topped by an inverted cone with an 8 mm diameter base. This cone base acts as a flame anchoring bluff body. These swirlers differ by the cone base height and, thus, by their effective outlet area which are 203.9 and 28.3 mm^2 for SW1 and SW2, respectively. This difference should be remarked in the central part of the swirler, in swirler 1 the bluff body surface has a height of 3 mm above the flow exit section whereas the swirler 2 cone is flush to the exit section. Considering the flow rate range used in this work, the Reynolds number, determined using the wetted perimeter of the swirler exit, lies between 753.5 and 8556.

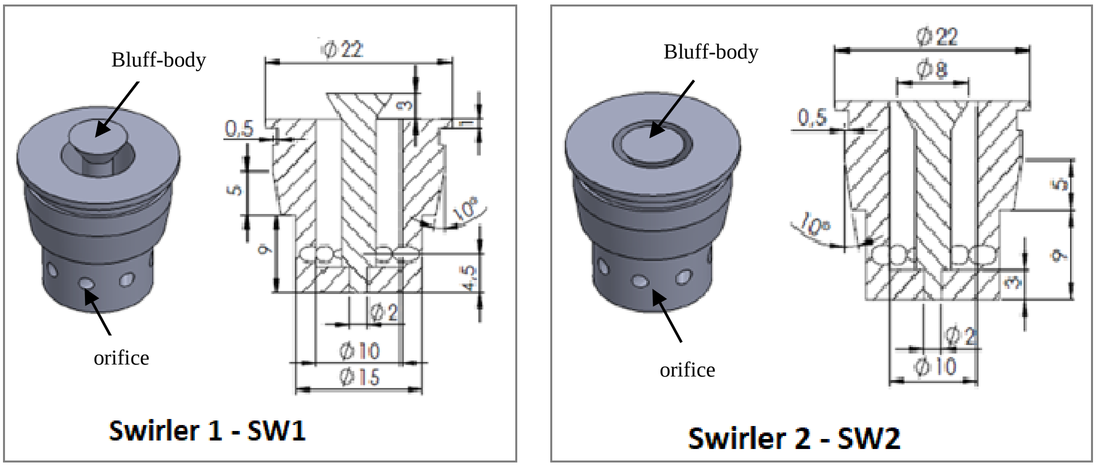

Figure 2. Studied swirler configurations: right heightened bluff body and left flush bluff body.

Figure 3 shows that the fuel/air mixture is introduced through a convergent located upstream to the swirlers. A honeycomb (not depicted) located inside the convergent section straightens and stabilizes the flow. The swirler is placed at the convergent section outlet and, at the top, the confinement is placed to limit the combustion chamber. As it may be seen in Fig. 3, the confinement consists of two main parts. The lower part is a stainless steel base where cooling water flows. The upper part contains four, 10 mm thickness, quartz windows that provide a lateral confinement of the combustion process. The quartz windows height is 170 mm. Two different confinement lateral dimensions are subject of this study: 30 and 40 mm. The quartz confinement is designed to provide ample optical access to the combustion region, thus allowing the use of laser-based diagnostic techniques, such as PIV or PLIF, that were employed in previous studies by (Cruz and Figueira, 2016), (Caetano and Figueira, 2015) and (Roque and Figueira, 2015).

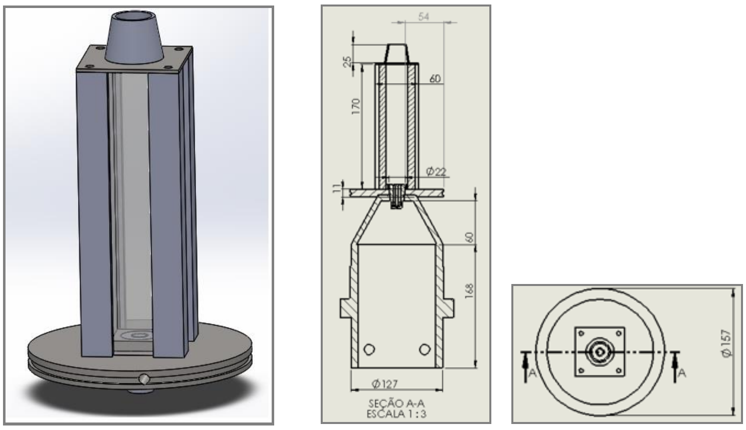

Figure 3. Scheme presented and the confinement configuration: left 3-D model - swirler, cooling base and confinement and right 2-D model - burner, swirler, cooling plate and confinement.

2.2 Combustion imaging

Time-integrated pan-spectral chemiluminescence images of the combustion process have been obtained by using a Canon EOS Rebel TS camera. This camera is fitted with a 58 mm diameter lens but without filters. All images presented here used f-11 aperture and an exposure time of 100 ms. Representative images have thus been obtained at various flow rates and equivalence ratios.

A LaVision Imager Intense CCD (Charge Coupled Device) camera, equipped with a 430 nm filter has been used to record flame images with an exposure time of 1 s and f-4 aperture. These chemiluminescence images are associated with the CH^* radical and, therefore, to the heat release zone of premixed flames. In order to evidence this region, the images have been deconvoluted using an Abel inversion technique which uses a Fourier-based algorithm (Pretzier, 1991) and (Pretzier, *et al.*, 1992). Such an inversion transforms the line-of-sight images to a cross-sectional representation assuming axial symmetry. For a given image, the centroid is first determined, then the deconvolution of both left and right positions are performed separately. The images presented in this work have been obtained using 24 terms in the Fourier expansion, which was found to be sufficient to represent the overall flame envelope.

3. RESULTS AND DISCUSSION

In this section, the flame topologies observed for each specific operating condition are first presented. These results allow determining a stability map of the combustion for this experimental setup. Concerning the turbulent flames, first the two different swirl geometries, SW1 and SW2 are analysed for the unconfined situation, then the influence of confinement dimension on the flame stabilization is assessed.

The nomenclature used to present the results is given in Tab. 1.

Table 1. Nomenclature used to represent the experimental devices and conditions.

LVE – D1	Lewis & Von Elbe (0.577 cm diameter tube)
LVE – D2	Lewis & Von Elbe (1.068 cm diameter tube)
SW1 – C	Swirler 1 confined
SW2 – C	Swirler 2 confined
SW1 – UC	Swirler 1 unconfined
SW2 – UC	Swirler 2 unconfined

The swirl intensity is usually characterized by swirl number (S), defined as the ratio between the axial flux of tangential momentum (G_h) and the axial momentum flux (G_z,) (Durox, *et al.*, 2013). Usually, the swirl number is expressed (Palmer, 1974) as

$$S = \frac{\int_0^R u_Z u_\theta r^2 dr}{R \int_0^R u_Z^2 r dr}, \tag{1}$$

where u_Z is the axial velocity and u_Θ is the azimuthal velocity, and R is the swirler radius. The area ratio (AR) is the ratio between the confinement area has been proposed by (Durox, *et al*., 2013), which approximates the fluid dynamical expression of Eq. (1) by using the geometrical features of the swirler. The geometrical swirl number and AR are given in Tab. 2.

Table 2. Geometric parameters of swirler and confinement.

	S	AR	
		Conf. 30 x 30 mm	Conf. 40 x 40 mm
SW1	1.88	13.6	24.3
SW2	0.26	31.8	56.6

3.1 Flame topologies

Two typical images of an unconfined flame are shown in Fig. 4. This figure allows to verify that the flame stabilizes either with a V shape near the swirler outlet or with an M shape. Below a critical Karlovitz number value the flame has an M shape and, in contrast, above this number the flame takes the form of V. This behaviour has also been observed by (Guiberti, *et al*., 2015), and will not be explored here.

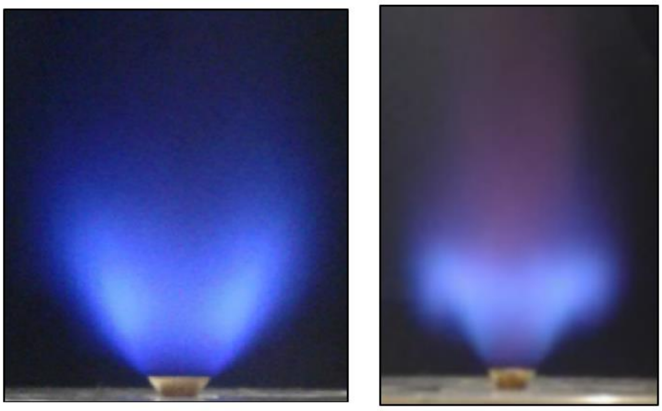

Figure 4. Unconfined swirling V flame (right) and swirling M flame (left).

Figure 5 compares average flame structures obtained in the unconfined and in the confined cases. This figure shows raw chemiluminescence images, obtained at 430 nm, and, also, the Abel deconvoluted 430 nm images. At the top of this figure (A), the unconfined flame clearly assumes a V shape. In contrast, the average confined flame is predominantly found at the vicinity of the combustor wall. Note that these flames correspond to identical values of mixture flow rate and composition.

(A)	**SW1 – UC**	
Φ = 1.5	(a) 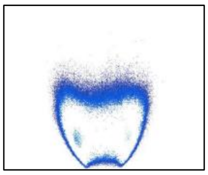	(b) 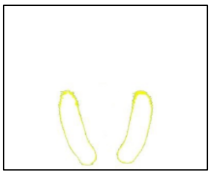
% CH_4 = 13.4		
Q (cm^3/s) = 500.1		
(B)	**SW1 – C (30 x 30 mm)**	
Φ = 1.3	(a) 	(b) 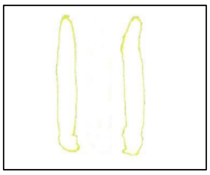
% CH_4 = 11.8		
Q (cm^3/s) = 566.8		

Figure 5. Unconfined swirling flame with SW1 swirler (A) and confined swirling flame with SW1 swirler (B); (a) chemiluminescence images and (b) Abel-deconvoluted chemiluminescence images.

The flame topology within the combustor is also influenced by the mixture composition, the confinement area ratio, and the swirl number. This is illustrated in Fig. 6, by pan-spectral chemiluminescence camera images for different swirlers, combustion chamber confinement area ratios and several mixtures composition features. In general, mixtures with larger equivalence ratios and smaller flow rates, which are far from blow-off, seem to interact with the combustor walls. On the other hand, at the vicinity of blow-off, e.g., for $\phi = 0.8$ and SW1 – C (40 x 40 mm^2), an elongated V-shaped flame results. Such an elongated flame has always been observed at the blow-off vicinity. For this particular value of equivalence ratio ($\phi = 0.8$) decreasing the swirl number leads to a shortened flame, i.e., going from SW1 – C to SW2 – C.

Comparing now, in Fig. 6, the same swirler (SW2 – C) images, it is possible to evidence the confinement area ratio influence. Indeed, this influence is particularly striking near the blow-off ($\phi = 0.8$), since reducing the area ratio leads the flame to change from an elongated V-shape to one that strongly interacts with the wall. It is thus expected that the blow-off equivalence ratio will be smaller for smaller area ratios.

Φ	1.5	1.3	1.1	0.9	0.8
% CH_4	13.8	11.8	10.3	9.1	8.2
Q (cm^3/s)	483.5	566.8	650.1	733.5	816.8
SW1 – C (40 x 40 mm)					
SW2 – C (40 x 40 mm)					
SW2 – C (30 x 30 mm)		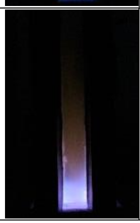			

Figure 6. Pan spectral camera images as a function of the mixture equivalence ratio for a given methane volume flow rate, for two different confinement area ratios.

3.2 Blow off limits

The results obtained in this study are compared to those of classical laminar Bunsen flames presented by (Lewis and Elbe, 1987), as shown in Fig. 7 and Fig. 8, where the blow-off limits are given in terms of mixture volume flow rate and methane/air ratio. In these figures, stable flames are found to occur for CH_4 concentrations above the curves. Note that, for laminar flames stabilized on a Bunsen burner, the blow-off methane concentration increases with the total flow rate and decreases with the tube diameter. This behaviour is associated to the velocity gradient at the tube wall and, thus, to the Karlovitz number.

3.2.1 Swirl number influence, unconfined flames

Figure 7 gives the measured blow-off limits for both swirlers as a function of the mixture volume flow rate and composition. For most of the operational range, blow-off occurs for rich fuel-air mixtures (methane/air stoichiometry corresponding to 9.5 %). This is possibly an undesirable feature for practical applications.

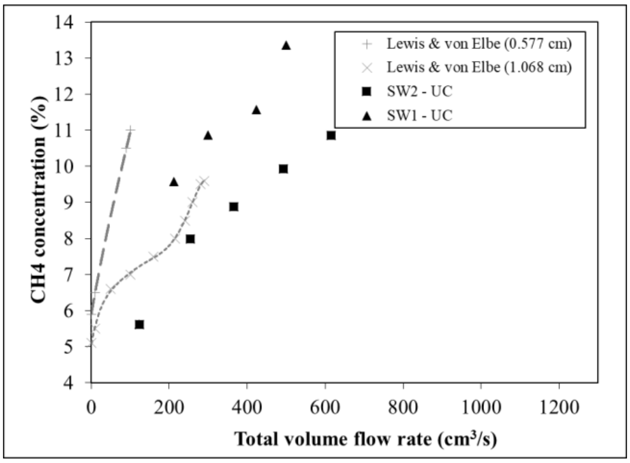

Figure 7. Blow-off limits of unconfined methane /air flames for two different geometries SW1 and SW2.

Figure 7 compares the results obtained for the two unconfined swirlers, SW1 – UC and SW2 – UC, and shows significant differences. Indeed, for a given mixture concentration, the blow-off flow rate of SW2-UC is larger than that of SW1 – UC. This larger operational envelope, in terms of blow-off, for SW2 – UC, seems to be associated with the smaller swirl number. Indeed, for a given mixture flow rate, a smaller swirl number should lead to a larger axial velocity component, u_Z, due to the smaller exit area. The azimuthal velocity component, u_Θ, is expected to be controlled by the orifice arrangement, which is the same for both swirlers. This larger value of u_Z should lead to a bluff body recirculating region with a larger pressure deficit with respect to the external flow. It is this hypothesized mechanism that could be responsible for the observed blow-off trends.

3.2.2 Confinement influence

Figure 8 compares the blow-off limits obtained with the two swirlers and the two confinements. A comparison with the results given in Fig. 7 allows to verify that the confined flames blow-off always occurs for lean mixtures, which is in marked contrast with respect to the unconfined flames. Furthermore, the CH_4 volume fraction at the blow-off decreases when the confinement cross section is reduced from 4x4 cm^2 to 3x3 cm^2. In particular, the minimum blow-off methane concentration is of 4.5 % for the smallest area ratio. The results given in Fig. 8 could be separated in three regimes:

1. Small flow rate regime ($Q < 400$ cm^3/s), when increasing the mixture flow rate leads to a decrease of blow-off equivalence ratio. This behavior could be explained by an increased flame/wall interaction as the turbulent flame brush volume increases.

2. Moderate flow rate regime ($400 < Q < 800$ cm^3/s), where the blow-off limits increase with the total volume flow rate. Such an increase seems to be similar to that observed for unconfined flames. In this moderate flow rate regime, the swirler details are found not to exert a considerable influence on the blow-off limit.

3. Large flow rate regime ($Q > 800$ cm^3/s). In this regime, the experimentally determined blow-off equivalence ratio is found to exhibit a large scatter for the largest confinement, with significant discrepancies amongst the swirlers (not shown here). The exact reasons controlling such a behavior are under investigations currently. It is likely that, for the V flame topology that arises at the blow-off vicinity, minute changes of the controlling parameters (flow rates) could lead to large deviations of the flame/wall interaction and, thus, of the blow-off limit.

It should be noted that the verified confinement influence is a direct consequence of flame/wall interactions. Such an influence has been observed by (Galley, *et al*., 2011), (Nogenmyr, *et al*., 2013), (Guiberti, *et al*., 2015), (Khalil, *et al*., 2016) and (Jourdaine, *et al*., 2016). Indeed, these studies indicate that strong flame wall interactions lead to a significant pre-heating of the fresh mixture and to the recirculation of hot combustion products. Both these effects reduce the combustion characteristic chemical time thus, increasing the stability range of the combustion chamber.

Although flash back of the flame in the burner is not the focus of the present investigation, it is worth noting that such a phenomenon has not been observed for the various flow rates and mixture compositions used.

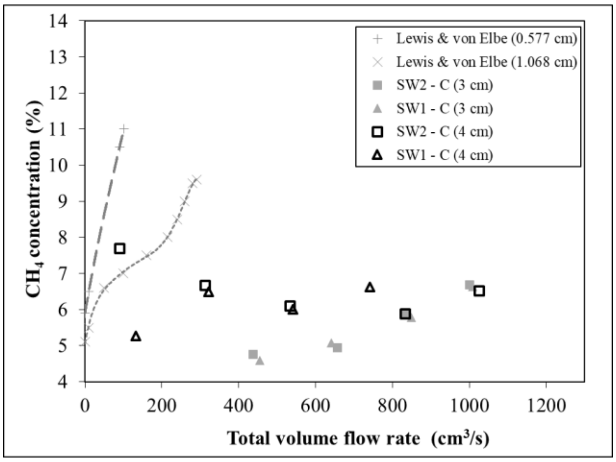

Figure 8. Blow-off limits of methane /air flames for two different confinements.

4. CONCLUSIONS

This work has presented a characterization of a novel premixed turbulent swirling combustion test bench. This characterization was based on panchromatic and filtered chemiluminescence imaging which allowed to identify flame shapes that arise under different operational conditions, swirl geometries and confinement area ratios.

A study of the blow-off limits identified the crucial role played by the confinement area ratio and, to a lesser extent, the swirl number. Smaller area ratios lead to a significant decrease of the blow-off equivalence ratio for a given mixture flow rate. In particular, the blow-off methane volume fraction was found to be as small as 4.5%, which amounts to a significant increase on the burner operational envelope.

Future work will involve the use of PIV and PLIF techniques to assess detailed turbulent flame structures. This experimental setup will also be adapted to burn prevaporized ethanol or butanol mixtures with air, thus allowing to investigate the turbulent combustion characteristics of these environmentally friendly fuels.

5. ACKNOWLEDGEMENTS

This work was supported by PUC-Rio and Laboratoire EM2C CNRS, CentraleSupélec, France.

6. REFERENCES

Bourgouin, J., Moeck, J., Durox, D., Schuller, T. and Candel, S., 2013. “Sensitivity of swirling flows to small changes in the swirler geometry”. *Comptes Rendus Mécanique*. Vol. 341, no. 1–2, pp. 211–219.

Caetano, N. R., & Figueira da Silva, L. F., 2015. “A comparative experimental study of turbulent non premixed flames stabilized by a bluff-body burner”. *Experimental Thermal and Fluid Science*. Vol. 63, pp. 20–33.

Candel, S., Durox, D., Schuller, T., Bourgouin, J. and Moeck, J.P., 2014. “Dynamics of swirling flames”. *Annual Review of Fluid Mechanics*. Vol. 46, pp. 147–173.

Chterev, I., Foley, C.W., Foti, D., Kostka, S., Caswell, A.W., Jiang, N., Lynch, A., Noble, D.R., Menon, S., Seitzman, J.M. and Lieuwen, T., 2014. “Flame and Flow Topologies in an Annular Swirling Flow”. *Combustion, Science and Technology*. Vol. 186, no. 8, pp. 1041–1074.

Cruz Villanueva, J. J., and Figueira da Silva, L. F., 2016. “Study of the Turbulent Velocity Field in the Near Wake of a Bluff Body. Flow”. *Turbulence and Combustion*. Vol. 97(3), pp. 715–728.

Daguse, T., Croonenbroek, T., Rolon, J.C., Darabiha, N. and Soufiani, A., 1996. “Study of radiative effects on laminar counterflow H_2/O_2N_2 diffusion flames”. *Combustion and Flame.* Vol. 106, no. 3, pp. 271–287.

Durox, D., Moeck, J.P., Bourgouin, J. F., Morenton, P., Viallon, M., Schuller, T. and Candel, T., 2013. "Flame dynamics of a variable swirl number system and instability control". *Combustion and Flame*. Vol. 160, no. 9, pp. 1729–1742.

Ebi, D. and Clemens, N.T., 2016. "Experimental investigation of upstream flame propagation during boundary layer flashback of swirl flames". *Combustion and Flame.* Vol. 168, pp. 39–52.

Foley, C.W., Chterev, I., Seitzman, J. and Lieuwen, T., 2015. "High Resolution Particle Image Velocimetry and CH-PLIF Measurements and Analysis of a Shear Layer Stabilized Flame". *Journal of Engineering for Gas Turbines and Power.* Vol. 138, no. 3, p. 31603.

Galley, D., Ducruix, S., Lacas, F. and Veynante, D., 2011. "Mixing and stabilization study of a partially premixed swirling flame using laser induced fluorescence". *Combustion and Flame*. Vol. 158, no. 1, pp. 155–171.

Guiberti, T.F., Durox, D., Zimmer, L. and Schuller, T., 2015. "Analysis of topology transitions of swirl flames interacting with the combustor side wall". *Combustion and Flame.* Vol. 162, no. 11, pp. 4342–4357.

Huang, Y. and Yang, V., 2009. "Dynamics and stability of lean-premixed swirl-stabilized combustion". Progress in Energy and Combustion Science. Vol. 35, no. 4. pp. 293–364.

Jourdaine, P., Mirat, C., Beaunier, J., Caudal, J., Joumani, Y. and Schuller, T., 2016. "Effect of Quarl on N_2- and CO_2-Diluted Methane Oxy-Flames Stabilized by an Axial-Plus-Tangential Swirler". In *Volume 4A: Combustion, Fuels and Emissions.* P. V04AT04A048.

Khalil, A.E.E., Brooks, J.M. and Gupta, A.K., 2016. "Impact of confinement on flowfield of swirl flow burners". *Fuel.* Vol. 184, pp. 1–9.

Kröner, M., Stelmayer, T., Fritz, J., Kiesewetter, F. and Hirsch, C., 2007. "Flame propagation in swirling flows - effect of local extinction on the combustion induced vortex breakdown". *Combustion, Science and Technology.* Vol. 179, no. 7, pp. 1385–1416.

Lewis, B., and Von Elbe, G., 1987. *Combustion, flames, and explosions of gases*. Academic Press, London, 3nd edition.

Nogenmyr, K., Cao, H., Chan, C.K. and Cheng, R.K., 2013. "Effects of confinement on premixed turbulent swirling flame using large Eddy simulation". *Combustion Theory Model.* vol. 17, no. 6, pp. 1003–1019.

Orbay, R.C., Nogenmyr, K.J., Klingmann, J., and Bai, X.S., 2013. "Swirling turbulent flows in a combustion chamber with and without heat release". *Fuel.* Vol. 104, pp. 133–146.

Palmer, H., 1974. *Combustion Technology : Some Modern Developments*. Elsevier Science.

Pretzier, G., Jäger, H., Neger, T., Philipp, H., & Woisetschläger, J., 1992. "Comparison of Different Methods of Abel Inversion Using Computer Simulated and Experimental Side-On Data". *Z. Naturforsch*. Vol 47a, pp. 955–970.

Roque Ccacya, A. O., and Figueira da Silva, L. F., 2015. "Characterization of multi-jet turbulent flames in cross flow using stereo-PIV and OH-PLIF". *Fire Safety Journal*. Vol. 78, pp. 44–54.

Sayad, P., Schönborn, A., Li M. and Klingmann, J., 2014. "Visualization of Different Flashback Mechanisms for H_2 /CH_4 Mixtures in a Variable-Swirl Burner". *Journal of Engineering for Gas Turbines and Power.* Vol. 137, no. 3, p. 31507.

Terhaar, S., Oberleithner, K. and Paschereit, C.O., 2014. "Impact of Steam-Dilution on the Flame Shape and Coherent Structures in Swirl-Stabilized Combustors". *Combustion, Science and Technology*. Vol. 186, no. 7, pp. 889–911.

7. RESPONSIBILITY NOTICE

The authors are the only responsible for the printed material included in this paper.